© 2017 IJSRSET | Volume 3 | Issue 5 | Print ISSN: 2395-1990 | Online ISSN : 2394-4099
Themed Section: Engineering and Technology

Advance in Penny-shaped cracks of piezoelectricity

Yi Xiao
Research School of Engineering, Australian National University, Acton, ACT 2601, Australia

ABSTRACT

This paper presents an overview of Penny-shaped cracks of piezoelectric materials. Developments of Penny-shaped crack problems in piezoelectric materials are presented. Finally, a brief summary of the approaches discussed is provided and future trends in this field are identified.

Keywords: Piezoelectric materials, Penny-shaped crack, piezoelectric cylinder

I. INTRODUCTION

Piezoelectric material is such that when it is subjected to a mechanical load, it generates an electric charge. This effect is usually called the "piezoelectric effect". Conversely, when piezoelectric material is stressed electrically by a voltage, its dimension change. This phenomenon is known as the "inverse piezoelectric effect". The study of piezoelectricity was initiated by J. and P. Curie in 1880 [1]. They found that certain crystalline materials generate an electric charge proportional to a mechanical stress. Since then new theories and applications of the field have been constantly advanced [2-10]. Voigt [2] developed the first complete and rigorous formulation of piezoelectricity in 1890. Since then several books on the phenomenon and theory of piezoelectricity have been written. Among them are the references by Cady [3], Tiersten [4], Parton and Kudryavtsev [5], Ikeda [6], Rogacheva [7], Qin [8-11], and Qin and Yang [12]. The first of these [2] treated the physical properties of piezoelectric crystals as well as their practical applications, the second [3] dealt with the linear equations of vibrations in piezoelectric materials, and the third and fourth [4, 5] gave a more detailed description of the physical properties of piezoelectricity. Rogacheva [7] presented general theories of piezoelectric shells. Qin [8-11] discussed Green's functions, advanced theory, and fracture mechanics of piezoelectric materials as well as applications to bone remodelling. Micromechanics of the piezoelectricity were discussed in [12]. These advances have resulted in a great number of publications including journal and conference papers. These include but not limit to applications to Branched crack problems[13-15], experimental investigation of bone materials [16-21], multi-field problems of bone remodelling [22-29], decay analysis of dissimilar laminates [30], moving crack problems [31], anti-plane crack problems [32, 33], fibre-pull out [34], fibre-push out [35-37], problems of frog Sartorius muscles [38], effective property evaluation [39-42], Green's function analysis [43-50], derivation of general solutions [51-55], boundary element analysis [56-63], micro-macro crack interaction problems [64], Trefftz finite element analysis [65-70], crack-inclusion problems [71, 72], crack growth problem [73, 74], multi-crack problems [75], crack-interface problems [76-78], closed crack-tip analysis [79], crack-path selection [80], penny-shaped crack analysis [81, 82], logarithmic singularity analysis [83], multi-layer piezoelectric actuator [84, 85], Symplectic mechanics analysis [86], fibre-reinforced composites [87], interlayer stress analysis [88], coupled thermo-electro-chemo-mechanical analysis [89], and damage analysis [90, 91].

Based on the analysis above, the present review consists of three major sections. Problems of an infinite piezoelectric material with a penny-shaped crack are discussed in Section 2. Section 3 focuses on solutions of a penny-shaped crack in a piezoelectric strip. Section 4 presents solutions for a penny-shaped crack in a piezoelectric cylinder. Finally, a brief summary on these sections is provided and areas that need further research are identified.

II. An infinite piezoelectric material with a penny-shaped crack

All formulations in this section are taken from the work of Lin et al [92]. In their paper, they consider an infinite piezoelectric ceramic containing a penny-shaped crack of radius a under axisymmetric electromechanical loads (Fig. 1). We discuss here analytical solutions, rather than numerical solutions of engineering problems [93-107]. For convenience, a cylindrical coordinate system (r, θ, z) originating at the center of the crack is used, with the z -axis perpendicular to the crack plane. The piezoelectric material is assumed to be transversely isotropic with the poling direction parallel to the z -axis and hexagonal symmetry. It is subjected to the far-field of a normal stress, $\sigma_z = \sigma_\infty$ and a uniform electric displacement $D_z = D_\infty$.

The constitutive equations for piezoelectric materials which are transversely isotropic and poled along the z-axis can be written as[8]

$$\sigma_{\theta\theta} = c_{12}u_{r,r} + c_{11}\frac{u_r}{r} + c_{13}u_{z,z} + e_{31}\phi_{,z} \quad (1)$$

$$\sigma_{zz} = c_{13}u_{r,r} + c_{13}\frac{u_r}{r} + c_{33}u_{z,z} + e_{33}\phi_{,z} \quad (2)$$

$$\sigma_{rr} = c_{11}u_{r,r} + c_{12}\frac{u_r}{r} + c_{13}u_{z,z} + e_{31}\phi_{,z} \quad (3)$$

$$\sigma_{rz} = c_{55}(u_{z,r} + u_{r,z}) + e_{15}\phi_{,r} \quad (4)$$

$$D_r = e_{15}(u_{z,r} + u_{r,z}) - \kappa_{11}\phi_{,r} \quad (5)$$

$$D_z = e_{31}(u_{r,r} + \frac{u_r}{r}) + e_{33}u_{z,z} - \kappa_{33}\phi_{,z} \quad (6)$$

The governing equations can then be expressed in terms of displacements and electric potential as

$$c_{11}\left(u_{r,rr} + \frac{u_{r,r}}{r} - \frac{u_r}{r^2}\right) + c_{55}u_{r,zz} + (c_{13}+c_{44})u_{z,rz} + (e_{31}+e_{15})\phi_{,rz} = 0 \quad (7)$$

$$(c_{13}+c_{55})\left(u_{r,rz} + \frac{u_{r,z}}{r}\right) + c_{33}u_{z,zz} + c_{55}\left(u_{z,rr} + \frac{u_{z,r}}{r}\right) + e_{15}\left(\phi_{,rr} + \frac{\phi_{,r}}{r}\right) + e_{33}\phi_{,zz} = 0 \quad (8)$$

$$(e_{31}+e_{15})\left(u_{r,rz} + \frac{u_{r,z}}{r}\right) + e_{15}\left(u_{z,rr} + \frac{u_{z,r}}{r}\right) + e_{33}u_{z,zz} - \kappa_{11}\left(\phi_{,rr} + \frac{\phi_{,r}}{r}\right) - \kappa_{33}\phi_{,zz} = 0 \quad (9)$$

The electric field components may be written in terms of an electric potential $\phi(r,z)$ as

$$E_r = -\phi_{,r}, \quad E_z = -\phi_{,z} \quad (10)$$

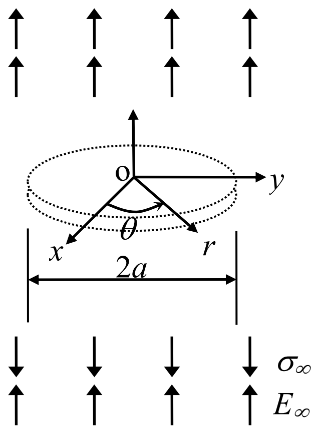

Fig. 1 A penny-shaped crack embedded in an infinite piezoelectric material

In a vacuum, the constitutive equations (5) and (6) and the governing equation (9) become

$$D_r = \kappa_0 E_r, \quad D_z = \kappa_0 E_z \quad (11)$$

$$\phi_{,rr} + \frac{\phi_{,r}}{r} + \phi_{,zz} = 0 \quad (12)$$

The problem of determining the distribution of stress and electric displacement in the vicinity of the crack is then equivalent to that of finding the distribution of stress and electric displacement in the semi-infinite piezoelectric material $z \geq 0,\ 0 \leq r \leq \infty$, subjected to the following boundary conditions:

$$\sigma_{zr}(r,0) = 0, \ (0 \leq r < \infty); \quad \sigma_{zz}(r,0) = 0, \ (0 \leq r < a); \quad u_z(r,0) = 0, \ (a \leq r < \infty) \quad (13)$$

$$E_r(r,0) = E_r^c(r,0), \ D_z(r,0) = D_z^c(r,0), \quad (0 \leq r < a); \quad \phi(r,0) = 0, \ (a \leq r < \infty)$$

(14)

$$\sigma_{zz}(r,z) = \sigma_\infty, \quad E_z(r,z) = E_\infty \quad (z \to \infty) \ (15)$$

where E_r^c and D_z^c are respectively the electric field and electric displacement in the void inside the crack. The far-field normal stress can be expressed in terms of E_∞ as

$$\sigma_\infty = \sigma_0 - \frac{(c_{11}+c_{12})e_{33} - 2c_{13}e_{31}}{c_{11}+c_{12}} E_\infty \quad (16)$$

where σ_0 is a uniform normal stress for a closed-circuit condition with the potential forced to remain zero.

The solution to the boundary value problem stated above is as follows [92]:

Assume that the solutions u_r, u_z and ϕ are of the form

$$u_r(r,z) = \frac{2}{\pi}\sum_{j=1}^{3}\int_0^\infty a_j A_j(\alpha)\exp(-\mu_j \alpha z)J_1(\alpha r)d\alpha + a_\infty r \quad (17)$$

$$u_z(r,z) = \frac{2}{\pi}\sum_{j=1}^{3}\int_0^\infty \frac{1}{\mu_j} A_j(\alpha)\exp(-\mu_j \alpha z)J_0(\alpha r)d\alpha + b_\infty z \quad (18)$$

$$\phi(r,z) = -\frac{2}{\pi}\sum_{j=1}^{3}\int_0^\infty \frac{b_j}{\mu_j} A_j(\alpha)\exp(-\mu_j \alpha z)J_0(\alpha r)d\alpha - c_\infty z \quad (19)$$

where $A_j(\alpha)$ $(j=1,2,3)$ are the unknowns to be solved, μ_j (j=1,2,3) are the roots of the characteristic equation [8], and J_0( ) and J_1( ) are the zero and first order Bessel functions of the first kind, respectively. The real constants a_∞, b_∞ and c_∞ can be obtained by applying far-field loading conditions as

$$\begin{aligned} a_\infty &= \frac{c_{13}\sigma_\infty + (c_{13}e_{33} - c_{33}e_{31})E_\infty}{2c_{13}^2 - c_{33}(c_{11}+c_{12})} \\ b_\infty &= \frac{-(c_{11}+c_{12})\sigma_\infty + [2c_{13}e_{31} - (c_{11}+c_{12})e_{33}]E_\infty}{2c_{13}^2 - c_{33}(c_{11}+c_{12})} \\ c_\infty &= E_\infty \end{aligned} \quad (20)$$

The constants a_j and b_j are

$$\begin{aligned} a_j &= \frac{(e_{31}+e_{15})(c_{33}\mu_j^2 - c_{55}) - (c_{13}+c_{55})(e_{33}\mu_j^2 - e_{15})}{(c_{55}\mu_j^2 - c_{11})(e_{33}\mu_j^2 - e_{15}) + (c_{13}+c_{55})(e_{31}+e_{15})\mu_j^2} \\ b_j &= \frac{(c_{55}\mu_j^2 - c_{11})a_j + (c_{13}+c_{55})}{e_{31}+e_{15}} \end{aligned} \quad (21)$$

To determine the coefficients A_j, applying the Fourier transform to Eq (12) we have

$$\phi^c = \frac{2}{\pi}\int_0^\infty C(\alpha)\sinh(\alpha z)J_0(\alpha r)d\alpha \quad (0 \le r < a) \quad (22)$$

where the superscript c stands for the variable is associated with the void inside the crack, and $C(\alpha)$ is unknown. Thus, the boundary conditions $(13)_1$ and (14) yield the following relations between unknown functions:

$$\begin{aligned} \frac{f_1}{\mu_1}A_1(\alpha) + \frac{f_2}{\mu_2}A_2(\alpha) + \frac{f_3}{\mu_3}A_3(\alpha) = 0 \\ \frac{b_1}{\mu_1}A_1(\alpha) + \frac{b_2}{\mu_2}A_2(\alpha) + \frac{b_3}{\mu_3}A_3(\alpha) = 0 \end{aligned} \quad (23)$$

where

$$f_j = c_{55}(a_j\mu_j^2 + 1) - e_{15}b_j \quad (j=1,2,3) \quad (24)$$

Making use of the mixed boundary conditions **Error! Reference source not found.**$_{2,3}$, we have

$$\begin{aligned} &\int_0^\infty \alpha F D(\alpha)J_0(\alpha r)d\alpha = -\frac{\pi}{2}\sigma_\infty \quad (0 \le r < a) \\ &\int_0^\infty D(\alpha)J_0(\alpha r)d\alpha = 0 \quad (a \le r < \infty) \end{aligned} \quad (25)$$

where

$$\begin{aligned} &D(\alpha) = \frac{A_1(\alpha)}{d_1} = \frac{A_2(\alpha)}{d_2} = \frac{A_3(\alpha)}{d_3}, \quad F = \sum_{j=1}^{3} g_j d_j, \\ &d_1 = \mu_1(b_2 f_3 - b_3 f_2), \quad d_2 = \mu_2(b_3 f_1 - b_1 f_3), \\ &d_3 = \mu_3(b_1 f_2 - b_2 f_1), \; g_j = c_{13}a_j - c_{33} + e_{33}b_j \; (j=1,2,3) \end{aligned} \quad (26)$$

It is noted from Eq (26) that $D(\alpha)$ is the only unknown in Eq (25). The set of dual integral (25) may be obtained by using a new function $\Psi(\xi)$ defined by

$$D(\alpha) = -\frac{a^2\sigma_\infty}{F}\int_0^1 \Psi(\xi)\sin(a\alpha\xi)d\xi \quad (27)$$

Having satisfied Eq (25) for $a \le r < \infty$, the remaining condition for $0 \le r < a$ leads to an Able integral equation for $\Psi(\xi)$. The solution for $\Psi(\xi)$ is expressed by

$$\Psi(\xi) = \xi \quad (28)$$

The displacements and electric potential near the crack border are then obtained as

$$\begin{aligned} u_r &= \frac{K_I\sqrt{r_1}}{F}\sum_{j=1}^{3} a_j d_j \left\{\left(\cos^2\theta_1 + \mu_j^2\sin^2\theta_1\right)^{1/2} + \cos\theta_1\right\}^{1/2} \\ u_z &= -\frac{K_I\sqrt{r_1}}{F}\sum_{j=1}^{3} \frac{d_j}{\mu_j} \left\{\left(\cos^2\theta_1 + \mu_j^2\sin^2\theta_1\right)^{1/2} - \cos\theta_1\right\}^{1/2} \\ u_z &= \frac{K_I\sqrt{r_1}}{F}\sum_{j=1}^{3} \frac{b_j d_j}{\mu_j} \left\{\left(\cos^2\theta_1 + \mu_j^2\sin^2\theta_1\right)^{1/2} - \cos\theta_1\right\}^{1/2} \end{aligned} \quad (29)$$

where the polar coordinates r_1 and θ_1 are defined as

$$r_1 = \left\{(r-a)^2 + z^2\right\}^{1/2}, \quad \theta_1 = \tan^{-1}\left(\frac{z}{r-a}\right) \quad (30)$$

Substituting Eq (29) into the constitutive equations (1)-(6), we obtain the singular parts of the stress and electric displacements in the neighborhood of the crack border as

$$\sigma_{rr} = \frac{K_I}{2F\sqrt{r_1}}\sum_{j=1}^{3} m_j d_j R_j^c(\theta_1), \sigma_{zz} = \frac{K_I}{2F\sqrt{r_1}}\sum_{j=1}^{3} g_j d_j R_j^c(\theta_1),$$
$$\sigma_{rr} = -\frac{K_I}{2F\sqrt{r_1}}\sum_{j=1}^{3}\frac{f_j d_j}{\mu_j} R_j^s(\theta_1) \quad (31)$$

$$D_r = -\frac{K_I}{2F\sqrt{r_1}}\sum_{j=1}^{3}\frac{n_j d_j}{\mu_j} R_j^s(\theta_1), \quad D_z = \frac{K_I}{2F\sqrt{r_1}}\sum_{j=1}^{3} h_j d_j R_j^c(\theta_1)$$

(32)

where

$$h_j = e_{31}a_j + e_{33} - \kappa_{33}b_j, \quad m_j = c_{11}a_j - c_{13} + e_{31}b_j, \quad (j = 1,2,3) \quad n_j = e_{15}(\mu_j^2 a_j + 1) + \kappa_{11}b_j \quad (33)$$

The stress intensity factor K_I for the crack model is obtained as

$$K_I = \lim_{r\to a^+} \sigma_{zz}(r,0)\sqrt{2(r-a)} = \frac{2}{\pi}\sigma_\infty\sqrt{a} \quad (34)$$

The electric displacement intensity factor K_D is given by

$$K_D = \lim_{r\to a^+} D_z(r,0)\sqrt{2(r-a)} = \left(\frac{1}{F}\sum_{j=1}^{3} h_j d_j\right)K_I \quad (35)$$

III. A penny-shaped crack in a piezoelectric strip

In this section we present a brief review of the results given in [108]. Consider a piezoelectric layer with a penny-shaped crack of radius a as shown in Fig. 2.

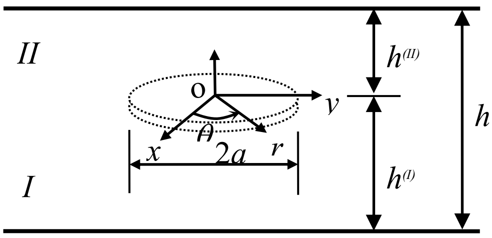

Fig. 2 A piezoelectric strip with a penny-shaped crack

For the sake of convenience, Eqs (17)-(19) are rewritten in the form

$$\mathbf{U} = \int_0^\infty F(\alpha)((A_1 J_1(\alpha r),\ A_3 J_0(\alpha r), A_4 J_0(\alpha r))e^{\mu\alpha z} d\alpha \quad (36)$$

where U={u_r, u_z, ϕ}^{T}, $F(\alpha)$ is an unknown function to be determined, μ and A_j are eigenvalue and eigenvector respectively [10] which is rewritten as follows:

$$\begin{bmatrix} c_{11} - c_{55}\mu^2 & (c_{13}+c_{55})\mu & (e_{31}+e_{15})\mu \\ (c_{13}+c_{55})\mu & c_{33}\mu^2 - c_{55} & e_{33}\mu^2 - e_{15} \\ (e_{31}+e_{15})\mu & e_{33}\mu^2 - e_{15} & \kappa_{11} - \kappa_{33}\mu^2 \end{bmatrix} \begin{Bmatrix} A_1 \\ A_3 \\ A_4 \end{Bmatrix} = 0 \quad (37)$$

In terms of these eigenvalues and eigenvectors, a general expression for the displacements and electric potential can be written as

$$\mathbf{U} = \int_0^\infty [G(\alpha r)][A(z)][\{F\}d\alpha \quad (38)$$

where

$$[G(\alpha r)] = \text{diag}[J_1(\alpha r),\ J_1(\alpha r),\ J_1(\alpha r)], \quad [F] = \{F_\beta\}^T,$$
$$[A(z)] = \begin{bmatrix} A_{k\beta}e^{\alpha\mu_\beta z} \\ A_{4\beta}e^{\alpha\mu_\beta z} \end{bmatrix}, \quad k = 1,3;\ \beta = 1,2,3,4,5,6 \quad (39)$$

Substituting Eq (38) into the constitutive equations (2), (4), and (6) yields

$$\{T(r,z)\} = \begin{Bmatrix} \sigma_{rz} \\ \sigma_{zz} \\ D_z \end{Bmatrix} = \int_0^\infty \alpha[G(\alpha r)][B]\{F\}d\alpha \quad (40)$$

where

$$B_{1\beta}(z) = (c_{55}\mu_\beta A_{1\beta} - c_{55}A_{3\beta} - e_{15}A_{4\beta})e^{\alpha\mu_\beta z}$$
$$B_{2\beta}(z) = (c_{13}A_{1\beta} + c_{33}\mu_\beta A_{3\beta} + e_{33}\mu_\beta A_{4\beta})e^{\alpha\mu_\beta z} \quad (41)$$
$$B_{3\beta}(z) = (e_{31}A_{1\beta} + e_{33}\mu_\beta A_{3\beta} - \kappa_{33}\mu_\beta A_{4\beta})e^{\alpha\mu_\beta z}$$

Noting that superscripts (I) and (II) represent the related variables associated with the materials occupying the lower and upper parts (see Fig. 2) and assuming that $\{t^{(0)}(r)\}$ represents $\{T^{(I)}(r, z^{(I)}=0)\}$ or $\{T^{(II)}(r, z^{(II)}=0)\}$, the boundary conditions can be rewritten as

$$\{T^{(I)}(r, z=-h^{(I)})\} = \{t^{(I)}(r)\},$$
$$\{T^{(II)}(r, z=h^{(II)})\} = \{t^{(II)}(r)\} \quad (42)$$

The mixed boundary conditions along the crack line are

$$\{t(r)\} = \{t^{(0)}(r)\}, \quad r < a;$$
$$\{U^{(I)}(r, z=0)\} = \{U^{(II)}(r, z=0)\}, \quad r \ge a \quad (43)$$

The unknown vector $\{F\}$ can be expressed in terms of $\{t^{(i)}(r)\}$, (i=0,I,II) by utilizing the inverse Hankel transform to Eq (40) as

$$\{F^{(I)}\} = \left[C^{(I)}\right]\begin{Bmatrix}\Gamma^{(0)}(\alpha) \\ \Gamma^{(I)}(\alpha)\end{Bmatrix}, \quad \{F^{(II)}\} = \left[C^{(II)}\right]\begin{Bmatrix}\Gamma^{(II)}(\alpha) \\ \Gamma^{(0)}(\alpha)\end{Bmatrix} \quad (44)$$

where $\Gamma^{(i)}(\alpha)$, $(i = 0, I, II)$ is the Hankel transform of $\{t^{(i)}(r)\}$, and

$$\{C^{(I)}\} = \begin{bmatrix} B(0) \\ B(-h^{(I)}) \end{bmatrix}^{-1}, \quad \{C^{(II)}\} = \begin{bmatrix} B(h^{(II)}) \\ B(0) \end{bmatrix}^{-1} \tag{45}$$

Substituting Eq (44) into Eq (38), we obtain

$$\{U^{(I)}\} = \int_0^\infty [G(\alpha r)[D_1^{(I)}\ D_2^{(I)}]\begin{Bmatrix} \Gamma^{(0)}(\alpha) \\ \Gamma^{(I)}(\alpha) \end{Bmatrix} d\alpha,$$
$$\{U^{(II)}\} = \int_0^\infty [G(\alpha r)[D_1^{(II)}\ D_2^{(II)}]\begin{Bmatrix} \Gamma^{(II)}(\alpha) \\ \Gamma^{(0)}(\alpha) \end{Bmatrix} d\alpha \tag{46}$$

where

$$[D_1^{(I)}\ D_2^{(I)}] = [A^{(I)}(y)][C^{(I)}],\ [D_1^{(II)}\ D_2^{(II)}] = [A^{(II)}(y)][C^{(II)}] \tag{47}$$

are two 4×4 matrices.

Making use of the continuity condition (43), we have

$$\int_0^\infty [G(\alpha r)]([L]\{\Gamma^{(I)}\} + [M]\{\Gamma^{(0)}\} + [N]\{\Gamma^{(II)}\})d\alpha = 0, \quad r \geq a \tag{48}$$

where

$$[L(\alpha)] = [D_2^{(I)}(0)],\ [M(\alpha)] = [D_1^{(I)}(0)] - [D_2^{(II)}(0)],$$
$$[N(\alpha)] = -[D_1^{(II)}(0)] \tag{49}$$

From Eq (47), the solution of $\Gamma(\alpha)$ can be expressed in terms of an unknown vector $\{d(r)\} = \{d_{u_r}(r), d_{u_z}(r), d_\phi(r)\}^T$ as

$$[M]\{\Gamma^{(0)}\} = -[L]\{\Gamma^{(I)}\} - [N]\{\Gamma^{(II)}\} + \alpha^{1/2}\int_0^a \begin{Bmatrix} d_{u_r} J_{3/2}(\alpha r) \\ d_{u_z} J_{1/2}(\alpha r) \\ d_\phi J_{1/2}(\alpha r) \end{Bmatrix} dr \tag{50}$$

Define $[K(\alpha)] = [M(\alpha)]^{-1} - [M(\infty)]^{-1}$, then it follows from Eq (50) that

$$\{\Gamma^{(0)}\} = -\{\Gamma_b(\alpha)\} + ([M(\infty)]^{-1} + [K(\alpha)])\alpha^{1/2}\int_0^a \begin{Bmatrix} d_{u_r}(x) J_{3/2}(\alpha x) \\ d_{u_z}(x) J_{1/2}(\alpha x) \\ d_\phi(x) J_{1/2}(\alpha x) \end{Bmatrix} dx \tag{51}$$

where

$$[\Gamma_b(\alpha)] = [M(\alpha)]^{-1}[L]\{\Gamma^{(I)}(\alpha)\} + [M(\infty)]^{-1}[N]\{\Gamma^{(II)}(\alpha)\} \tag{52}$$

The solution of $\{d(r)\}$ can be obtained by substituting the crack surface condition (43) into Eq (51):

$$[M(\infty)]^{-1}\int_0^\infty \left(\alpha^{3/2}[G(\alpha r)\int_0^a \begin{Bmatrix} d_{u_r}(x) J_{3/2}(\alpha x) \\ d_{u_z}(x) J_{1/2}(\alpha x) \\ d_\phi(x) J_{1/2}(\alpha x) \end{Bmatrix} dx \right) d\alpha,\ r < a$$
$$+\int_0^\infty \left(\alpha^{3/2}[G(\alpha r)[K(\alpha)]\int_0^a \begin{Bmatrix} d_{u_r}(x) J_{3/2}(\alpha x) \\ d_{u_z}(x) J_{1/2}(\alpha x) \\ d_\phi(x) J_{1/2}(\alpha x) \end{Bmatrix} dx \right) d\alpha = \sigma_b(r) \tag{53}$$

where

$$\sigma_b(r) = \{t^{(0)}(r)\} + \int_0^\infty \alpha[G(\alpha r)]\{\Gamma_b[\alpha]\}d\alpha \tag{54}$$

Eq (53) can be used for solving $\{d(r)\}$ numerically. Once $\{d\}$ is solved from Eq (53), the stress and electric displacement intensity factors can be calculated using the following equation:

$$\{K\} = \sqrt{2(r-a)}\{t(r)\}_{r\to a^+} = -\sqrt{\frac{2a}{\pi}}[M(\infty)]^{-1}\{d(a)\} \tag{55}$$

The displacement and electric potential jumps between the upper and lower faces of the crack can be calculated from (46) and (50) as

$$\Delta\{U\} = \{U^{(II)}(r,0)\} - \{U^{(I)}(r,0)\} = -\int_0^a \int_0^\infty \alpha^{1/2}[G(\alpha r)] \begin{Bmatrix} d_{u_r} J_{3/2}(\alpha r) \\ d_{u_z} J_{1/2}(\alpha r) \\ d_\phi J_{1/2}(\alpha r) \end{Bmatrix} drd\alpha \tag{56}$$

Integration of Eq **Error! Reference source not found.** with respect to α yields

$$\Delta\{U\} = -\sqrt{\frac{2}{\pi}}\int_r^a \begin{Bmatrix} d_{u_r}(x)\sqrt{r}/x \\ d_{u_z}(x)/\sqrt{x} \\ d_\phi(x)/\sqrt{x} \end{Bmatrix} \frac{1}{\sqrt{x^2 - r^2}} dx \tag{57}$$

IV.A penny-shaped crack in a piezoelectric cylinder

In this section, the developments in [82] for the response of elastic stress and electric displacement in a long piezoelectric cylinder with a centered penny-shaped crack are presented. The long piezoelectric cylinder is subjected to two types of boundary conditions: (i) the piezoelectric cylinder is inserted in a smooth rigid bore of radius b, (ii) the surface of the piezoelectric cylinder is stress and electric charge free. Based on the potential function approach and Hankel transform, a system of dual integral equations is obtained, and then re-duced to a Fredholm integral equation of the second kind.

The constitutive equations are defined in Eqs (1)-(6). The equilibrium equation and the equation of electrostatics for this problem are given as

$$\sigma_{rr,r} + \sigma_{rz,z} + \frac{\sigma_{rr} - \sigma_{\theta\theta}}{r} = 0,$$
$$\sigma_{rz,r} + \sigma_{zz,z} + \frac{\sigma_{rz}}{r} = 0, \tag{58}$$
$$D_{r,r} + D_{z,z} + \frac{D_r}{r} = 0$$

In the derivation of the analytic solution, the following potential functions are introduced [109, 110]:

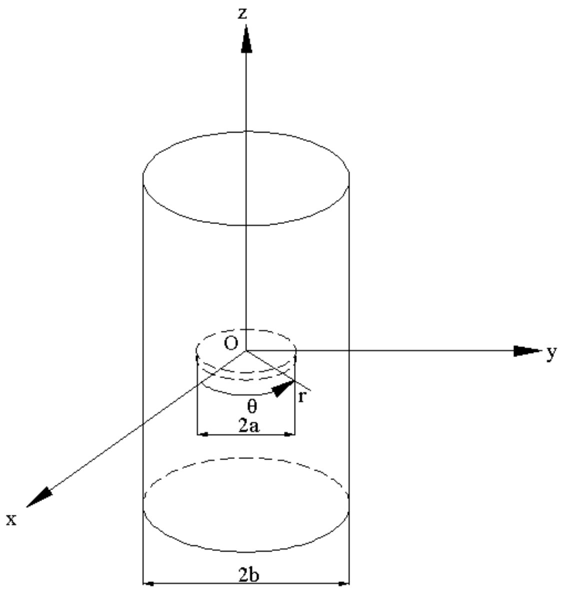

Fig. 3 Penny-shaped crack in a piezoelectric cylinder

$$u_r = \frac{\partial \Phi}{\partial r}, \quad u_z = k_1 \frac{\partial \Phi}{\partial z}, \quad \phi = -k_2 \frac{\partial \Phi}{\partial z} \qquad (59)$$

where $\Phi(r, z)$ is the potential function, and k_1 and k_2 are unknown constants to be determined.

Substituting Eq (59) into Eqs (1)-(6), and then into Eq (58), we have

$$\Phi_{,rr} + \frac{1}{r}\Phi_{,r} + n\Phi_{,zz} = 0 \qquad (60)$$

where

$$n = \frac{c_{44} + (c_{13} + c_{44})k_1 - (e_{31} + e_{15})k_2}{c_{11}} = \frac{c_{33}k_1 - e_{33}k_2}{c_{44}k_1 + c_{13} + c_{44} - e_{15}k_2} = \frac{e_{33}k_1 + \kappa_{33}k_2}{e_{15}k_1 + e_{15} + e_{31} + \kappa_{11}k_2} \qquad (61)$$

According the principle of superposition, the governing equation (60) becomes

$$\sum_{i=1}^{3}[\Phi_{i,rr} + \frac{1}{r}\Phi_{i,rr} + \Phi_{i,z_i z_i}]$$

or

$$c_{11}\sum_{i=1}^{3}(\frac{\partial \Phi_i}{\partial r^2} + \frac{1}{r}\frac{\partial \Phi_i}{\partial r}) + \sum_{i=1}^{3}\{[c_{55} + k_{1i}(c_{13} + c_{55}) + k_{2i}(e_{31} + e_{15})]\frac{\partial \Phi_i}{\partial z^2}\} = 0,$$
$$\sum_{i=1}^{3}\{[c_{44}k_{1i} + c_{13} + c_{55} + e_{15}k_{2i}](\frac{\partial \Phi_i}{\partial r^2} + \frac{1}{r}\frac{\partial \Phi_i}{\partial r}) + [c_{33}k_{1i} + e_{33}k_{2i}]\frac{\partial \Phi_i}{\partial z^2}\} = 0,$$
$$\sum_{i=1}^{3}\{[e_{15}k_{1i} + e_{31} + e_{15} - d_{11}k_{2i}](\frac{\partial \Phi_i}{\partial r^2} + \frac{1}{r}\frac{\partial \Phi_i}{\partial r}) + [e_{33}k_{1i} - d_{33}k_{2i}]\frac{\partial \Phi_i}{\partial z^2}\} = 0 \qquad (62)$$

where $z_i = z/\sqrt{n_i} = \mu_i z$, μ_i are the roots of the characteristic equation [8] and $\Phi_i(r, z)$ $(i = 1,2,3)$ are the corresponding potential functions. The displacement and electric potential equations are then in the form

$$u_r = \sum_{1}^{3}\frac{\partial \Phi_i}{\partial r}, \quad u_z = \sum_{i=1}^{3}k_{1i}\frac{\partial \Phi_i}{\partial z}, \quad \phi = -\sum_{i=1}^{3}k_{2i}\frac{\partial \Phi_i}{\partial z} \qquad (63)$$

where k_{1i} and k_{2i} ($i = 1,2,3$) are determined from Eq (61).

Following the procedure presented in [109], we take the solution of the Eq (62) in the form:

$$\Phi_i(r, z) = \int_0^\infty \frac{1}{\xi}\left[A_i(\xi)I_0(\frac{\xi r}{\mu_i})\cos(\xi z) + B_i(\xi)\exp(-\xi\mu_i z)J_0(\xi r)\right]d\xi \qquad (64)$$

where $A_i(\xi)$, $B_i(\xi)$, $(i = 1,2,3)$ are the unknown functions to be determined.

Then we have expressions of the components of displacement, stress and electric displacement in the following form:

$$u_z(r, z) = -\sum_{i=1}^{3}k_{1i}\int_0^\infty A_i(\xi)I_0(\frac{\xi r}{\mu_i})\sin(\xi z)d\xi - \sum_{i=1}^{3}k_{1i}s_i\int_0^\infty B_i(\xi)J_0(\xi r)e^{-\xi\mu_i z}d\xi + \bar{a}(r)z \qquad (65)$$

$$u_r(r, z) = \sum_{i=1}^{3}\frac{1}{\mu_i}\int_0^\infty A_i(\xi)I_1(\frac{\xi r}{\mu_i})\cos(\xi z)d\xi - \sum_{i=1}^{3}\int_0^\infty B_i(\xi)J_1(\xi r)e^{-\xi\mu_i z}d\xi \qquad (66)$$

$$\varphi(r, z) = \sum_{i=1}^{3}k_{2i}\int_0^\infty A_i(\xi)I_1(\frac{\xi r}{\mu_i})\sin(\xi z)d\xi + \sum_{i=1}^{3}k_{2i}s_i\int_0^\infty B_i(\xi)J_0(\xi r)e^{-\xi\mu_i z}d\xi - \bar{b}(r)z \qquad (67)$$

$$\sigma_z = -\sum_{i=1}^{3}\frac{F_{1i}}{\mu_i^2}\int_0^\infty \xi A_i(\xi)I_0(\frac{\xi r}{\mu_i})\cos(\xi z)d\xi + \sum_{i=1}^{3}F_{1i}\int_0^\infty \xi B_i(\xi)J_0(\xi r)e^{-\xi\mu_i z}d\xi + \bar{c}(r) \qquad (68)$$

$$\sigma_r = -\sum_{i=1}^{3}\frac{F_{5i}}{\mu_i^2}\int_0^\infty \xi A_i(\xi)I_0(\frac{\xi r}{\mu_i})\cos(\xi z)d\xi + \frac{c_{11} - c_{12}}{2}\sum_{i=1}^{3}\frac{1}{\mu_i^2}\int_0^\infty \xi A_i(\xi)I_2(\frac{\xi r}{\mu_i})\cos(\xi z)d\xi + \sum_{i=1}^{3}F_{5i}\int_0^\infty \xi B_i(\xi)J_0(\xi r)e^{-\xi\mu_i z}d\xi + \frac{c_{11} - c_{12}}{2}\sum_{i=1}^{3}\int_0^\infty \xi B_i(\xi)J_2(\xi r)e^{-\xi\mu_i z}d\xi \qquad (69)$$

$$\sigma_{zr} = -\sum_{i=1}^{3}\frac{F_{3i}}{\mu_i^2}\int_0^\infty \xi A_i(\xi)I_1(\frac{\xi r}{\mu_i})\sin(\xi z)d\xi + \sum_{i=1}^{3}F_{3i}\int_0^\infty \xi B_i(\xi)J_1(\xi r)e^{-\xi\mu_i z}d\xi \qquad (70)$$

$$D_z = -\sum_{i=1}^{3}\frac{F_{2i}}{\mu_i^2}\int_0^\infty \xi A_i(\xi) I_0(\frac{\xi r}{\mu_i})\cos(\xi z)d\xi + \sum_{i=1}^{3} F_{2i}\int_0^\infty \xi B_i(\xi)J_0(\xi r)e^{-\xi\mu_i z}d\xi + \bar{d}(r) \quad (71)$$

$$D_r = -\sum_{i=1}^{3}\frac{F_{4i}}{\mu_i^2}\int_0^\infty \xi A_i(\xi) I_1(\frac{\xi r}{\mu_i})\sin(\xi z)d\xi + \sum_{i=1}^{3} F_{4i}\int_0^\infty \xi B_i(\xi)J_1(\xi r)e^{-\xi\mu_i z}d\xi \quad (72)$$

where

$$F_{1i} = (c_{33}k_{1i} - e_{33}k_{2i})\mu_i^2 - c_{13}, \quad F_{2i} = (e_{33}k_{1i} + d_{33}k_{2i})\mu_i^2 - e_{31},$$
$$F_{3i} = \left[c_{44}(1+k_{1i}) - e_{15}k_{2i}\right]\mu_i, \quad F_{4i} = \left[e_{15}(1+k_{1i}) + d_{11}k_{2i}\right]\mu_i,$$
$$F_{5i} = (c_{13}k_{1i} - e_{31}k_{2i})\mu_i^2 - \frac{c_{11}+c_{12}}{2} \quad (73)$$

$$\bar{a}(r) = \frac{d_{33}\bar{\sigma}(r) + \bar{e}_{33}\bar{D}(r)}{c_{33}d_{33} + e_{33}^2}, \quad \bar{b}(r) = \frac{c_{33}\bar{D}(r) - e_{33}\bar{\sigma}(r)}{c_{33}d_{33} + e_{33}^2}, \quad (74)$$
$$\bar{c}(r) = \bar{\sigma}(r), \quad \bar{d}(r) = \bar{D}(r)$$

We consider separately two sets of boundary conditions.

Case 1: In the first case it is assumed that the piezoelectric cylindrical surface is free from shear and is supported in such a way that the radial component of the displacement vector vanishes on the surface. Such a situation would arise physically if the piezoelectric cylinder was embedded in a rigid cylindrical hollow (of exactly the same radius) and was then deformed by the application of a known stress and an electric displacement at the end of the piezoelectric cylinder. The problem of determining the distribution of stress and electric displacement in the vicinity of the crack is equivalent to that of finding the distribution of stress and electric displacement in the semi-infinite cylinder $z \ge 0$, $0 \le r \le a$, when its plane boundary $z = 0$ is subjected to the condition:

$$\sigma_z(r,0) = 0, \quad D_z(r,0^+) = D_z(r,0^-),$$
$$E_r(r,0^+) = E_r(r,0^+), \quad (0 \le r < a);$$
$$u_z(r,0) = 0, \quad \phi(r,0) = 0, \quad (a < r < b);$$
$$\sigma_{rz}(r,0) = 0, \quad (0 \le r < b) \quad (75)$$

and its curved boundary $r = b$ is subjected to the conditions:

$$u_r(b,z) = 0, \quad \sigma_{rz}(b,z) = 0, \quad D_r(b,z) = 0 \quad (76)$$

From the boundary conditions (75) and (76), and making use of the Fourier inversion theorem and the Hankel inversion theorem, we find that:

$$A_1(\xi) = \frac{1}{\Delta(\xi)}\sum_{i=1}^{3} N_{1i}(\xi) f_{1i}(\xi), \quad A_2(\xi) = \frac{1}{\Delta(\xi)}\sum_{i=1}^{3} N_{2i}(\xi) f_{2i}(\xi),$$
$$A_3(\xi) = \frac{1}{\Delta(\xi)}\sum_{i=1}^{3} N_{3i}(\xi) f_{3i}(\xi) \quad (77)$$

$$B_1(\xi) = M_1 B_1(\xi), \quad B_2(\xi) = M_2 B_1(\xi), \quad B_3(\xi) = M_3 B_1(\xi) \quad (78)$$

in which

$$M_1 = 1, \quad M_2 = \frac{F_{31}k_{23}\mu_3 - F_{33}k_{21}\mu_1}{F_{33}k_{22}\mu_2 - F_{32}k_{23}\mu_3}, \quad M_3 = \frac{F_{32}k_{21}\mu_1 - F_{31}k_{22}\mu_2}{F_{33}k_{22}\mu_2 - F_{32}k_{23}\mu_3} \quad (79)$$

$$f_i(\xi) = \frac{2}{\pi}\int_0^\infty \frac{\eta B_1(\eta)J_1(\eta b)}{\eta^2\mu_i^2 + \xi^2}d\eta, \quad f_{2i}(\xi) = \frac{2}{\pi}\int_0^\infty \frac{\eta^2 B_1(\eta)J_0(\eta b)}{\eta^2\mu_i^2 + \xi^2}d\eta,$$
$$f_{3i}(\xi) = \frac{2}{\pi}\int_0^\infty \frac{\eta^2 B_1(\eta)J_2(\eta b)}{\eta^2\mu_i^2 + \xi^2}d\eta \quad (80)$$

$$\Delta(\xi) = \left[h_{12}(\xi)h_{33}(\xi) - h_{32}(\xi)h_{13}(\xi)\right]h_{21}(\xi) + \left[h_{31}(\xi)h_{13}(\xi) - h_{11}(\xi)h_{33}(\xi)\right]h_{22}(\xi) + \left[h_{11}(\xi)h_{32}(\xi) - h_{31}(\xi)h_{12}(\xi)\right]h_{23}(\xi) \quad (81)$$

$$N_{1i}(\xi) = \left[(h_{13}(\xi)h_{22}(\xi) - h_{12}(\xi)h_{23}(\xi)\right]g_{3i} + \left[(h_{12}(\xi)h_{33}(\xi) - h_{13}(\xi)h_{32}(\xi)\right]g_{2i} + \left[(h_{23}(\xi)h_{32}(\xi) - h_{22}(\xi)h_{33}(\xi)\right]g_{1i} \quad (82)$$

$$N_{2i}(\xi) = \left[(h_{11}(\xi)h_{23}(\xi) - h_{21}(\xi)h_{13}(\xi)\right]g_{3i} + \left[(h_{13}(\xi)h_{31}(\xi) - h_{11}(\xi)h_{33}(\xi)\right]g_{2i} + \left[(h_{21}(\xi)h_{33}(\xi) - h_{31}(\xi)h_{23}(\xi)\right]g_{1i} \quad (83)$$

$$N_{3i}(\xi) = \left[(h_{12}(\xi)h_{21}(\xi) - h_{11}(\xi)h_{22}(\xi)\right]g_{3i} + \left[(h_{11}(\xi)h_{32}(\xi) - h_{31}(\xi)h_{12}(\xi)\right]g_{2i} + \left[(h_{22}(\xi)h_{31}(\xi) - h_{21}(\xi)h_{32}(\xi)\right]g_{1i} \quad (84)$$

with

$$h_{1i}(\xi) = \frac{F_{4i}}{\mu_i^2}I_1(\frac{\xi b}{\mu_i}), \quad g_{1i} = F_{4i}M_i, \quad h_{2i}(\xi) = \frac{F_{3i}}{\mu_i^2}I_1(\frac{\xi b}{\mu_i}),$$
$$g_{2i} = F_{3i}M_i\mu_i, \quad h_{3i}(\xi) = \frac{1}{\mu_i}I_1(\frac{\xi b}{\mu_i}), \quad g_{3i} = M_i\mu_i \quad (85)$$

From Eqs $(75)_{1,4}$, we can obtain a system of dual integral equations:

$$-\int_0^\infty \xi\left[\frac{F_{11}}{\mu_1^2}I_0(\frac{\xi r}{\mu_1})A_1(\xi) + \frac{F_{12}}{\mu_2^2}I_0(\frac{\xi r}{\mu_2})A_2(\xi) + \frac{F_{13}}{\mu_3^2}I_0(\frac{\xi r}{\mu_3})A_3(\xi)\right]d\xi + \int_0^\infty \xi\left[M_1F_{11} + M_2F_{12} + M_3F_{13}\right]B_1(\xi)J_0(\xi r)d\xi = -\bar{c}(r) \quad (0 \le r < a) \quad (86)$$

$$\int_0^\infty \left[M_1k_{11}s_1 + M_2k_{12}s_2 + M_3k_{13}s_3\right]B_1(\xi)J_0(\xi r)d\xi = 0 \quad (a < r < b) \quad (87)$$

Thess equations can be solved by using the function $\psi(\alpha)$, defined by

$$B_1(\xi) = \int_0^a \psi(\alpha)\sin(\xi\alpha)d\alpha \tag{88}$$

where $\psi(0) = 0$.

Using solutions of the following integrals:

$$\int_0^\infty \sin(sz)e^{-uz}dz = \frac{s}{s^2+u^2}, \quad \int_0^\infty \cos(sz)e^{-uz}dz = \frac{u}{s^2+u^2},$$

$$\int_0^t \frac{rI_0(\xi r)}{\sqrt{t^2-r^2}}dr = \frac{\sinh(\xi t)}{\xi}, \quad t<r$$

$$\int_0^\infty \frac{J_0(ru)\sin(ut)}{s^2+u^2}du = \frac{\sinh(st)K_0(rs)}{s}, \quad t<r$$

$$\int_0^\infty \frac{J_0(ru)\sin(ut)}{s^2+u^2}du = \frac{\sinh(st)K_0(rs)}{s}, \quad t<r$$

$$\int_0^\infty \frac{uJ_1(ru)\sin(ut)}{s^2+u^2}du = \sinh(st)K_1(rs), \quad t<r$$

$$\int_0^\infty \frac{u^2J_0(ru)\sin(ut)}{s^2+u^2}du = -s\cdot\sinh(st)K_0(rs), \quad t<r$$

$$\int_0^\infty \frac{u^2J_2(ru)\sin(ut)}{s^2+u^2}du = s\cdot\sinh(st)K_2(rs), \quad t<r$$

as well as the solution

$$f(t) = \frac{2\sin\pi\alpha}{\pi}\frac{d}{dt}\int_0^t \frac{ug(u)}{(t^2-u^2)^{1-\alpha}}du, \quad (a<t<b)$$

of the integral equation

$$\int_0^\infty \frac{f(t)}{(x^2-t^2)^\alpha}dt = g(x), \quad (0<\alpha<1, \quad a<x<b)$$

we can obtain a Fredholm integral equation of the second kind in the form

$$\psi(\alpha) + \int_0^a \psi(\beta)L(\alpha,\beta)d\beta = \frac{2}{\pi m_0}\int_0^\alpha \frac{r\bar{c}(r)}{\sqrt{\alpha^2-r^2}}dr \tag{89}$$

where

$$L(\alpha,\beta) = \frac{4}{\pi^2 m_0}\sum_{j=1}^3 \frac{F_{1j}}{\mu_j}\int_0^\infty \frac{1}{\Delta(\xi)}\sinh(\frac{\xi\alpha}{\mu_j}) \cdot\sum_{i=1}^3 \frac{1}{\mu_i^2}N_{ji}(\xi)\sinh(\frac{\xi\beta}{\mu_i})K_1(\frac{\xi b}{\mu_i})d\xi \tag{90}$$

Case 2: In the second case we assume that the piezoelectric cylindrical surface is stress free. The conditions (75) remain the same, and the boundary conditions (76) are replaced by the following conditions:

$$\sigma_{rr}(b,z)=0, \quad \sigma_{rz}(b,z)=0, \quad D_r(b,z)=0, \quad (z\ge 0) \tag{91}$$

Performing a procedure similar to that in Case 1, we have:

$$\begin{aligned}
A_1(\xi) &= \frac{1}{\Delta(\xi)}\sum_{i=1}^3\left[N_{1i}(\xi)f_{1i}(\xi)+P_{1i}(\xi)f_{2i}(\xi)+W_{1i}(\xi)f_{3i}(\xi)\right],\\
A_2(\xi) &= \frac{1}{\Delta(\xi)}\sum_{i=1}^3\left[N_{2i}(\xi)f_{1i}(\xi)+P_{2i}(\xi)f_{2i}(\xi)+W_{2i}(\xi)f_{3i}(\xi)\right],\\
A_3(\xi) &= \frac{1}{\Delta(\xi)}\sum_{i=1}^3\left[N_{3i}(\xi)f_{1i}(\xi)+P_{3i}(\xi)f_{2i}(\xi)+W_{3i}(\xi)f_{3i}(\xi)\right]
\end{aligned} \tag{92}$$

in which

$$\begin{aligned}
N_{1i}(\xi) &= \left[h_{52}(\xi)-h_{42}(\xi)\right]\left[h_{33}(\xi)g_{2i}-h_{23}(\xi)g_{3i}\right]\\
&\quad+\left[h_{53}(\xi)-h_{43}(\xi)\right]\left[h_{22}(\xi)g_{3i}-h_{32}(\xi)g_{2i}\right],\\
P_{1i}(\xi) &= \frac{1}{\xi}\left[h_{23}(\xi)h_{32}(\xi)-h_{22}(\xi)h_{33}(\xi)\right]g_{5i},\\
W_{1i}(\xi) &= \frac{1}{\xi}\left[h_{23}(\xi)h_{32}(\xi)-h_{22}(\xi)h_{33}(\xi)\right]g_{4i}
\end{aligned} \tag{93}$$

$$\begin{aligned}
N_{2i}(\xi) &= \left[h_{53}(\xi)-h_{43}(\xi)\right]\left[h_{31}(\xi)g_{2i}-h_{21}(\xi)g_{3i}\right]\\
&\quad+\left[h_{51}(\xi)-h_{41}(\xi)\right]\left[h_{23}(\xi)g_{3i}-h_{33}(\xi)g_{2i}\right],\\
P_{2i}(\xi) &= \frac{1}{\xi}\left[h_{21}(\xi)h_{33}(\xi)-h_{23}(\xi)h_{31}(\xi)\right]g_{5i},\\
W_{2i}(\xi) &= \frac{1}{\xi}\left[h_{21}(\xi)h_{33}(\xi)-h_{23}(\xi)h_{31}(\xi)\right]g_{4i}
\end{aligned} \tag{94}$$

$$\begin{aligned}
N_{3i}(\xi) &= \left[h_{51}(\xi)-h_{41}(\xi)\right]\left[h_{32}(\xi)g_{2i}-h_{22}(\xi)g_{3i}\right]\\
&\quad+\left[h_{52}(\xi)-h_{42}(\xi)\right]\left[h_{21}(\xi)g_{3i}-h_{31}(\xi)g_{2i}\right],\\
P_{3i}(\xi) &= \frac{1}{\xi}\left[h_{22}(\xi)h_{31}(\xi)-h_{21}(\xi)h_{32}(\xi)\right]g_{5i},\\
W_{3i}(\xi) &= \frac{1}{\xi}\left[h_{22}(\xi)h_{31}(\xi)-h_{21}(\xi)h_{32}(\xi)\right]g_{4i}
\end{aligned} \tag{95}$$

$$\begin{aligned}
\Delta(\xi) &= \left\{\left[-h_{53}(\xi)+h_{43}(\xi)\right]h_{32}(\xi)+\left[h_{52}(\xi)-h_{42}(\xi)\right]h_{33}(\xi)\right\}h_{21}(\xi)\\
&\quad+\left\{\left[h_{53}(\xi)-h_{43}(\xi)\right]h_{31}(\xi)+\left[-h_{51}(\xi)+h_{41}(\xi)\right]h_{33}(\xi)\right\}h_{22}(\xi)\\
&\quad+\left\{\left[h_{51}(\xi)-h_{41}(\xi)\right]h_{32}(\xi)+\left[-h_{52}(\xi)+h_{42}(\xi)\right]h_{31}(\xi)\right\}h_{23}(\xi)
\end{aligned} \tag{96}$$

with

$$h_{4i}(\xi) = \frac{c_{11}-c_{12}}{2}\frac{1}{\mu_i^2}I_2(\frac{\xi b}{\mu_i}), \quad g_{4i} = \frac{c_{11}-c_{12}}{2}M_i\mu_i \tag{97}$$

$$h_{5i}(\xi) = \frac{F_{5i}}{\mu_i^2}I_0(\frac{\xi b}{\mu_i}), \quad g_{5i} = F_{5i}M_i\mu_i \tag{98}$$

and the remaining steps are the same as those in Case 2.

Then we can obtain a Fredholm integral equation of the second kind which is exactly the same as that given in Eqs (86) and (87), except that the kernel $L(\alpha,\beta)$ takes the form:

$$L(\alpha,\beta) = \frac{4}{\pi^2 m_0}\sum_{j=1}^3\frac{F_{1j}}{\mu_j}\int_0^\infty \frac{1}{\Delta(\xi)}\sinh(\frac{\xi\alpha}{\mu_j})\sum_{i=1}^3\frac{1}{\mu_i^2}\sinh(\frac{\xi\beta}{\mu_i}) \times\left\{N_{ji}(\xi)K_1(\frac{\xi b}{\mu_i})-\frac{\xi}{\mu_i}P_{ji}(\xi)K_0(\frac{\xi b}{\mu_i})+\frac{\xi}{\mu_i}W_{ji}(\xi)K_2(\frac{\xi b}{\mu_i})\right\}d\xi \tag{99}$$

The field intensity factors are then expressed in the form

$$K_I = \lim_{r\to a^+} \sqrt{2\pi(r-a)}\sigma_{zz}(r,0) = \sqrt{\frac{\pi}{a}}m_0\psi(a),$$
$$K_D = \lim_{r\to a^+} \sqrt{2\pi(r-a)}D_z(r,0) = \sqrt{\frac{\pi}{a}}m_1\psi(a),$$
$$K_\varepsilon = \lim_{r\to a^+} \sqrt{2\pi(r-a)}\varepsilon_{zz}(r,0) = \sqrt{\frac{\pi}{a}}m_2\psi(a),$$
$$K_E = \lim_{r\to a^+} \sqrt{2\pi(r-a)}E_z(r,0) = \sqrt{\frac{\pi}{a}}m_3\psi(a) \quad (100)$$

in which

$$m_0 = -(M_1F_{11} + M_2F_{12} + M_3F_{13}),$$
$$m_1 = -(F_{21}M_1 + F_{22}M_2 + F_{23}M_3),$$
$$m_2 = -(k_{11}\mu_1^2M_1 + k_{12}\mu_1^2M_2 + k_{13}\mu_1^3M_3),$$
$$m_3 = -(k_{21}\mu_1^2M_1 + k_{22}\mu_2^2M_2 + k_{23}\mu_3^2M_3) \quad (101)$$

and K_I, K_D, K_ε, and K_E are the stress intensity factor, electric displacement intensity factor, strain intensity factor and electric field intensity factor, respectively.

V. CONCLUSIONS AND FUTURE DEVELOPMENTS

On the basis of the preceding discussion, following conclusions can be drawn. This review presents an overall view on Penny-shaped cracks of piezoelectric materials. It includes a penny-shaped crack in an infinite piezoelectric material, a piezoelectric strip, and a piezoelectric cylinder.

It is recognized that study on piezoelectric materials becomes a hot topic and has become increasingly popular due their widely applications in engineering fields. However, there are still many possible extensions and areas in need of further development in the future. Among those developments one could list the following:

1 Development of efficient Trefftz finite element-boundary element method schemes for complex piezoelectric structures and the related general purpose computer codes with preprocessing and postprocessing capabilities.

2 Applications of piezoelectric composites to MEMS and smart devices and development of the associated design and fabrication approaches.

3 Extension of the Trefftz-finite element method to elastodynamics of piezoelectric structures, dynamics of thin and thick plate bending and fracture mechanics for structures containing piezoelectric sensor and actuators.

4 Development of multiscale framework across from continuum to micro- and nano-scales for modeling piezoelectric materials and structures.

VI. REFERENCES

[1] J. Curie, P. Curie, Development par compression de l'eletricite polaire dans les cristaux hemiedres a faces inclines, Comptes Rendus Acad. Sci. Paris, 91 (1880) 294.

[2] W. Voigt, General theory of the piezo-and pyroelectric properties of crystals, Abh. Gott, 36(1) (1890).

[3] W. Cady, Piezoelectricity, vols. 1 and 2, Dover Publishers, New York, 1964.

[4] H.F. Tiersten, Linear piezoelectric plate vibrations, Springer, New York, 1969.

[5] V.Z. Parton, B.A. Kudryavtsev, Electromagnetoelasticity: piezoelectrics and electrically conductive solids, Gordon and Breach Science Publishers, New York, 1988.

[6] T. Ikeda, Fundamentals of piezoelectricity, Oxford university press, New York, 1996.

[7] N.N. Rogacheva, The theory of piezoelectric shells and plates, CRC Press, Boca Raton, 1994.

[8] Q.H. Qin, Fracture mechanics of piezoelectric materials, WIT Press, Southampton, 2001.

[9] Q.H. Qin, Green's function and boundary elements of multifield materials, Elsevier, Oxford, 2007.

[10] Q.H. Qin, Advanced mechanics of piezoelectricity, Higher Education Press and Springer, Beijing, 2013.

[11] Q.H. Qin, Mechanics of Cellular Bone Remodeling: Coupled Thermal, Electrical, and Mechanical Field Effects, CRC Press, Taylor & Francis, Boca Raton, 2013.

[12] Q.H. Qin, Q.S. Yang, Macro-micro theory on multifield coupling behaivor of hetereogenous materials, Higher Education Press and Springer, Beijing, 2008.

[13] S. Diao, Q.H. Qin, J. Dong, On branched interface cracks between two piezoelectric materials, Mechanics research communications, 23(6) (1996) 615-620.

[14] Q.H. Qin, Y.W. Mai, Crack branch in piezoelectric bimaterial system, International Journal of Engineering Science, 38(6) (2000) 673-693.

[15] Q.H. Qin, X. Zhang, Crack deflection at an interface between dissimilar piezoelectric materials, International Journal of Fracture, 102(4) (2000) 355-370.

[16] D. Fu, Z. Hou, Q.H. Qin, L. Xu, Y. Zeng, Influence of Shear Stress on Behaviors of Piezoelectric Voltages

in Bone, Journal of Applied Biomechanics, 28(4) (2012) 387-393.
[17] D.H. Fu, Z.D. Hou, Q.H. Qin, Analysis of the waveforms of piezoelectric voltage of bone, Journal of Tianjin University, 39 (2006) 349-353.
[18] D.H. Fu, Z.D. Hou, Q.H. Qin, Influence of a notch on the piezoelectric voltages in bone, Engineering Mechanics, 28(1) (2011) 233-237.
[19] D.H. Fu, Z.D. Hou, Q.H. Qin, C. Lu, On the Influence of Relative Humidity on Piezoelectric Signals in Bone, Journal of Experimental Mechanics, 24(5) (2009) 473-478.
[20] Z. Hou, D. Fu, Q.H. Qin, An exponential law for stretching–relaxation properties of bone piezovoltages, International Journal of Solids and Structures, 48(3) (2011) 603-610.
[21] L. Xu, Z. Hou, D. Fu, Q.-H. Qin, Y. Wang, Stretched exponential relaxation of piezovoltages in wet bovine bone, Journal of the Mechanical Behavior of Biomedical Materials, 41 (2015) 115-123.
[22] X. He, C. Qu, Q.H. Qin, A theoretical model for surface bone remodeling under electromagnetic loads, Archive of Applied Mechanics, 78(3) (2008) 163-175.
[23] Q.H. Qin, Thermoelectroelastic solutions for internal bone remodelling under constant loads, Mechanics of electromagnetic solids, 3 (2003) 73-88.
[24] Q.H. Qin, Multi-field bone remodeling under axial and transverse loads, in: D.R. Boomington (Ed.) New research on biomaterials, Nova Science Publishers, New York, 2007, pp. 49-91.
[25] Q.H. Qin, C. Qu, J. Ye, Thermoelectroelastic solutions for surface bone remodeling under axial and transverse loads, Biomaterials, 26(33) (2005) 6798-6810.
[26] Q.H. Qin, J.Q. Ye, Thermoelectroelastic solutions for internal bone remodeling under axial and transverse loads, International Journal of Solids and Structures, 41(9) (2004) 2447-2460.
[27] C. Qu, X. He, Q.H. Qin, Bone functional remodeling under multi-field loadings, Proceedings of the 5th Australasian Congress on Applied Mechanics, (2007) 627-632.
[28] C. Qu, Q.H. Qin, Bone remodeling under multi-field coupled loading, Zhineng Xitong Xuebao(CAAI Transactions on Intelligent Systems), 2(3) (2007) 52-58.
[29] C. Qu, Q.H. Qin, Y. Kang, A hypothetical mechanism of bone remodeling and modeling under electromagnetic loads, Biomaterials, 27(21) (2006) 4050-4057.
[30] X. He, J.S. Wang, Q.H. Qin, Saint-Venant decay analysis of FGPM laminates and dissimilar piezoelectric laminates, Mechanics of Materials, 39(12) (2007) 1053-1065.
[31] K.Q. Hu, Y.L. Kang, Q.H. Qin, A moving crack in a rectangular magnetoelectroelastic body, Engineering Fracture Mechanics, 74(5) (2007) 751-770.
[32] K.Q. Hu, Q.H. Qin, Y.L. Kang, Anti-plane shear crack in a magnetoelectroelastic layer sandwiched between dissimilar half spaces, Engineering Fracture Mechanics, 74(7) (2007) 1139-1147.
[33] Q.H. Qin, Solving anti-plane problems of piezoelectric materials by the Trefftz finite element approach, Computational Mechanics, 31(6) (2003) 461-468.
[34] H.Y. Liu, Q.H. Qin, Y.W. Mai, Theoretical model of piezoelectric fibre pull-out, International Journal of Solids and Structures, 40(20) (2003) 5511-5519.
[35] Q.H. Qin, J.S. Wang, Y.L. Kang, A theoretical model for electroelastic analysis in piezoelectric fibre push-out test, Archive of Applied Mechanics, 75(8-9) (2006) 527-540.
[36] J.S. Wang, Q.H. Qin, Debonding criterion for the piezoelectric fibre push-out test, Philosophical Magazine Letters, 86(2) (2006) 123-136.
[37] J.S. Wang, Q.H. Qin, Y.L. Kang, Stress and electric field transfer of piezoelectric fibre push-out under electrical and mechanical loading, in: Proc. of 9th International Conference on Inspection, Appraisal, Repairs & Maintenance of Structures, Fuzhou, China, 20-21 October, CI-Premier PTY LTD, ISBN: 981-05-3548-1, 2005, pp. 435-442.
[38] Z. Liu, Z. Hou, Q.H. Qin, Y. Yu, L. Tang, On electromechanical behaviour of frog sartorius muscles, in: Engineering in Medicine and Biology Society, 2005. IEEE-EMBS 2005. 27th Annual International Conference of the, IEEE, 2006, pp. 1252-1255.
[39] Q.H. Qin, Using GSC theory for effective thermal expansion and pyroelectric coefficients of cracked piezoelectric solids, International Journal of Fracture, 82(3) (1996) R41-R46.
[40] Q.H. Qin, Y.W. Mai, S.W. Yu, Effective moduli for thermopiezoelectric materials with microcracks, International Journal of Fracture, 91(4) (1998) 359-371.
[41] Q.H. Qin, S.W. Yu, Effective moduli of piezoelectric material with microcavities, International Journal of Solids and Structures, 35(36) (1998) 5085-5095.
[42] Q.H. Qin, S.W. Yu, Using Mori-Tanaka method for effective moduli of cracked thermopiezoelectric materials, in: ICF 9-Sydney, Australia-1997, 1997.

[43] Q.H. Qin, Thermoelectroelastic Green's function for a piezoelectric plate containing an elliptic hole, Mechanics of Materials, 30(1) (1998) 21-29.

[44] Q.H. Qin, Thermoelectroelastic Green’s function for thermal load inside or on the boundary of an elliptic inclusion, Mechanics of Materials, 31(10) (1999) 611-626.

[45] Q.H. Qin, Green's function for thermopiezoelectric plates with holes of various shapes, Archive of Applied Mechanics, 69(6) (1999) 406-418.

[46] Q.H. Qin, Green function and its application for a piezoelectric plate with various openings, Archive of Applied Mechanics, 69(2) (1999) 133-144.

[47] Q.H. Qin, Green's functions of magnetoelectroelastic solids with a half-plane boundary or bimaterial interface, Philosophical Magazine Letters, 84(12) (2004) 771-779.

[48] Q.H. Qin, 2D Green's functions of defective magnetoelectroelastic solids under thermal loading, Engineering Analysis with Boundary Elements, 29(6) (2005) 577-585.

[49] Q.H. Qin, Green’s functions of magnetoelectroelastic solids and applications to fracture analysis, in: Proc. of 9th International Conference on Inspection, Appraisal, Repairs & Maintenance of Structures, Fuzhou, China, 20-21 October,2005, CI-Premier PTY LTD, ISBN: 981-05-3548-1, 2005, pp. 93-106.

[50] Q.H. Qin, Y.W. Mai, Thermoelectroelastic Green's function and its application for bimaterial of piezoelectric materials, Archive of Applied Mechanics, 68(6) (1998) 433-444.

[51] Q.H. Qin, General solutions for thermopiezoelectrics with various holes under thermal loading, International Journal of Solids and Structures, 37(39) (2000) 5561-5578.

[52] Q.H. Qin, Y.W. Mai, A new thermoelectroelastic solution for piezoelectric materials with various openings, Acta Mechanica, 138(1) (1999) 97-111.

[53] Q.H. Qin, Y.W. Mai, S.W. Yu, Some problems in plane thermopiezoelectric materials with holes, International Journal of Solids and Structures, 36(3) (1999) 427-439.

[54] Q.H. Qin, A new solution for thermopiezoelectric solid with an insulated elliptic hole, Acta Mechanica Sinica, 14(2) (1998) 157-170.

[55] Q.H. Qin, General solutions for thermopiezoelectric materials with various openings, Encyclopedia of Thermal Stresses, (2014) 1932-1942.

[56] Q.H. Qin, Thermoelectroelastic analysis of cracks in piezoelectric half-plane by BEM, Computational Mechanics, 23(4) (1999) 353-360.

[57] Q.H. Qin, Material properties of piezoelectric composites by BEM and homogenization method, Composite structures, 66(1) (2004) 295-299.

[58] Q.H. Qin, Micromechanics-BE solution for properties of piezoelectric materials with defects, Engineering Analysis with Boundary Elements, 28(7) (2004) 809-814.

[59] Q.H. Qin, Micromechanics-BEM Analysis for Piezoelectric Composites, Tsinghua Science & Technology, 10(1) (2005) 30-34.

[60] Q.H. Qin, Boundary Element Method, in: J.S. Yang (Ed.) Special Topics in the Theory of Piezoelectricity, Springer, Cambridge Massachusetts, 2009, pp. 137-168.

[61] Q.H. Qin, Analysis of Piezoelectric Solids through Boundary Element Method, J Appl Mech Eng, 2(1) (2012) e113.

[62] Q.H. Qin, Y.W. Mai, BEM for crack-hole problems in thermopiezoelectric materials, Engineering Fracture Mechanics, 69(5) (2002) 577-588.

[63] Q.H. Qin, Mode III fracture analysis of piezoelectric materials by Trefftz BEM, Structural Engineering and Mechanics, 20(2) (2005) 225-240.

[64] Q.H. Qin, Thermopiezoelectric interaction of macro-and micro-cracks in piezoelectric medium, Theoretical and Applied Fracture Mechanics, 32(2) (1999) 129-135.

[65] Q.H. Qin, Variational formulations for TFEM of piezoelectricity, International Journal of Solids and Structures, 40(23) (2003) 6335-6346.

[66] Q.H. Qin, Fracture Analysis of Piezoelectric Materials by Boundary and Trefftz Finite Element Methods, WCCM VI in conjunction with APCOM’04, Sept. 5-10, 2004, Beijing, China, (2004).

[67] Q.H. Qin, Trefftz Plane Element of Piezoelectric Plate with p-Extension Capabilities, IUTAM Symposium on Mechanics and Reliability of Actuating Materials, (2006) 144-153.

[68] C. Cao, Q.H. Qin, A. Yu, Hybrid fundamental-solution-based FEM for piezoelectric materials, Computational Mechanics, 50(4) (2012) 397-412.

[69] C. Cao, A. Yu, Q.H. Qin, A new hybrid finite element approach for plane piezoelectricity with defects, Acta Mechanica, 224(1) (2013) 41-61.

[70] H. Wang, Q.H. Qin, Fracture analysis in plane piezoelectric media using hybrid finite element model, in: International Conference of fracture, 2013.

[71] Q.H. Qin, M. Lu, BEM for crack-inclusion problems of plane thermopiezoelectric solids, International Journal for Numerical Methods in Engineering, 48(7) (2000) 1071-1088.

[72] Q.H. Qin, Thermoelectroelastic solution for elliptic inclusions and application to crack–inclusion problems, Applied Mathematical Modelling, 25(1) (2000) 1-23.
[73] Q.H. Qin, Y.W. Mai, Crack growth prediction of an inclined crack in a half-plane thermopiezoelectric solid, Theoretical and Applied Fracture Mechanics, 26(3) (1997) 185-191.
[74] H.Y. Liu, Q.H. Qin, Y.W. Mai, Crack growth in composites with piezoelectric fibers, in: Proc. of the Third Int. Conf. for Mesomechanics, Xi'an, China, June 13-16, Tsinghua Univ. Press, Vol. 1, 2000, pp. 357-366.
[75] Q.H. Qin, Y.W. Mai, Multiple cracks in thermoelectroelastic bimaterials, Theoretical and Applied Fracture Mechanics, 29(2) (1998) 141-150.
[76] Q.H. Qin, Y.W. Mai, Thermal analysis for cracks near interfaces between piezoelectric materials, Localized Damage 1998: Fifth International Conference on Damage and Fracture Mechanics, (1998) 13-22.
[77] Q.H. Qin, S.W. Yu, An arbitrarily-oriented plane crack terminating at the interface between dissimilar piezoelectric materials, International Journal of Solids and Structures, 34(5) (1997) 581-590.
[78] Q.H. Qin, S.W. Yu, On the plane piezoelectric problem of a loaded crack terminating at a material interface, Acta Mechanica Solida Sinica, 9 (1996) 151-158.
[79] Q.H. Qin, Y.W. Mai, A closed crack tip model for interface cracks in thermopiezoelectric materials, International Journal of Solids and Structures, 36(16) (1999) 2463-2479.
[80] Q.H. Qin, Y.W. Mai, Crack path selection in piezoelectric bimaterials, Composite structures, 47(1) (1999) 519-524.
[81] Q.H. Qin, J.S. Wang, X. Li, Effect of elastic coating on fracture behaviour of piezoelectric fibre with a penny-shaped crack, Composite structures, 75(1) (2006) 465-471.
[82] J.S. Wang, Q.H. Qin, Penny-shaped Crack in a Solid Piezoelectric Cylinder With Two Typical Boundary Conditions, Journal of Beijing University of Technology, 32(S1) (2006) 29-34.
[83] Q.H. Qin, S. Yu, Logarithmic singularity at crack tips in piezoelectric media, Chinese science bulletin, 41(7) (1996) 563-566.
[84] W. Qiu, Y. Kang, Q. Sun, Q.H. Qin, Y. Lin, Stress analysis and geometrical configuration selection for multilayer piezoelectric displacement actuator, Acta Mechanica Solida Sinica, 17(4) (2004) 323-329.
[85] W. Qiu, Y.L. Kang, Q.H. Qin, Q. Sun, F. Xu, Study for multilayer piezoelectric composite structure as displacement actuator by Moire interferometry and infrared thermography experiments, Materials Science and Engineering: A, 452 (2007) 228-234.
[86] J.S. Wang, Q.H. Qin, Symplectic model for piezoelectric wedges and its application in analysis of electroelastic singularities, Philosophical Magazine, 87(2) (2007) 225-251.
[87] C.-Y. Lee, Q.H. Qin, G. Walpole, Numerical modeling on electric response of fibre-orientation of composites with piezoelectricity, International Journal of Research and Reviews in Applied Science, 16(3) (2013) 377-386.
[88] Q.S. Yang, Q.H. Qin, T. Liu, Interlayer stress in laminate beam of piezoelectric and elastic materials, Composite structures, 75(1) (2006) 587-592.
[89] Q.S. Yang, Q.H. Qin, L. Ma, X. Lu, C. Cui, A theoretical model and finite element formulation for coupled thermo-electro-chemo-mechanical media, Mechanics of Materials, 42(2) (2010) 148-156.
[90] S.W. Yu, Q.H. Qin, Damage analysis of thermopiezoelectric properties: Part I—crack tip singularities, Theoretical and Applied Fracture Mechanics, 25(3) (1996) 263-277.
[91] S.W. Yu, Q.H. Qin, Damage analysis of thermopiezoelectric properties: Part II. Effective crack model, Theoretical and Applied Fracture Mechanics, 25(3) (1996) 279-288.
[92] S. Lin, F. Narita, Y. Shindo, Electroelastic analysis of a penny-shaped crack in a piezoelectric ceramic under mode I loading, Mechanics Research Communications, 30(4) (2003) 371-386.
[93] H. Wang, Q.H. Qin, Fundamental-solution-based hybrid FEM for plane elasticity with special elements, Computational Mechanics, 48(5) (2011) 515-528.
[94] H. Wang, Q.H. Qin, Fundamental-solution-based finite element model for plane orthotropic elastic bodies, European Journal of Mechanics-A/Solids, 29(5) (2010) 801-809.
[95] M. Dhanasekar, J. Han, Q.H. Qin, A hybrid-Trefftz element containing an elliptic hole, Finite Elements in Analysis and Design, 42(14) (2006) 1314-1323.
[96] Q.H. Qin, C.X. Mao, Coupled torsional-flexural vibration of shaft systems in mechanical engineering—I. Finite element model, Computers & Structures, 58(4) (1996) 835-843.
[97] Q.H. Qin, Hybrid Trefftz finite-element approach for plate bending on an elastic foundation, Applied Mathematical Modelling, 18(6) (1994) 334-339.
[98] Q.H. Qin, The Trefftz finite and boundary element method, WIT Press, Southampton, 2000.
[99] Q.H. Qin, Trefftz finite element method and its applications, Applied Mechanics Reviews, 58(5) (2005) 316-337.

[100] Q.H. Qin, Hybrid-Trefftz finite element method for Reissner plates on an elastic foundation, Computer Methods in Applied Mechanics and Engineering, 122(3-4) (1995) 379-392.
[101] H. Wang, Q.H. Qin, Hybrid FEM with fundamental solutions as trial functions for heat conduction simulation, Acta Mechanica Solida Sinica, 22(5) (2009) 487-498.
[102] Q.H. Qin, H. Wang, Matlab and C programming for Trefftz finite element methods, New York: CRC Press, 2008.
[103] J. Jirousek, Q.H. Qin, Application of hybrid-Trefftz element approach to transient heat conduction analysis, Computers & Structures, 58(1) (1996) 195-201.
[104] Q.H. Qin, X.Q. He, Variational principles, FE and MPT for analysis of non-linear impact-contact problems, Computer methods in applied mechanics and engineering, 122(3) (1995) 205-222.
[105] Y. Cui, J. Wang, M. Dhanasekar, Q.H. Qin, Mode III fracture analysis by Trefftz boundary element method, Acta Mechanica Sinica, 23(2) (2007) 173-181.
[106] W.-G. Jiang, R.-Z. Zhong, Q.H. Qin, Y.-G. Tong, Homogenized Finite Element Analysis on Effective Elastoplastic Mechanical Behaviors of Composite with Imperfect Interfaces, International Journal of Molecular Sciences, 15(12) (2014) 23389-23407.
[107] H.-W. Wang, Q.H. Qin, H. Ji, Y. Sun, Comparison Among Different Modeling Techniques of 3D Micromechanical Modeling of Damage in Unidirectional Composites, Advanced Science Letters, 4(2) (2011) 400-407.
[108] B.-L. Wang, N. Noda, J.-C. Han, S.-Y. Du, A penny-shaped crack in a transversely isotropic piezoelectric layer, European Journal of Mechanics-A/Solids, 20(6) (2001) 997-1005.
[109] J. Yang, K. Lee, Penny shaped crack in a three-dimensional piezoelectric strip under in-plane normal loadings, Acta Mechanica, 148(1-4) (2001) 187-197.
[110] J.H. Yang, K.Y. Lee, Penny shaped crack in a piezoelectric cylinder surrounded by an elastic medium subjected to combined in-plane mechanical and electrical loads, International journal of solids and structures, 40(3) (2003) 573-590.